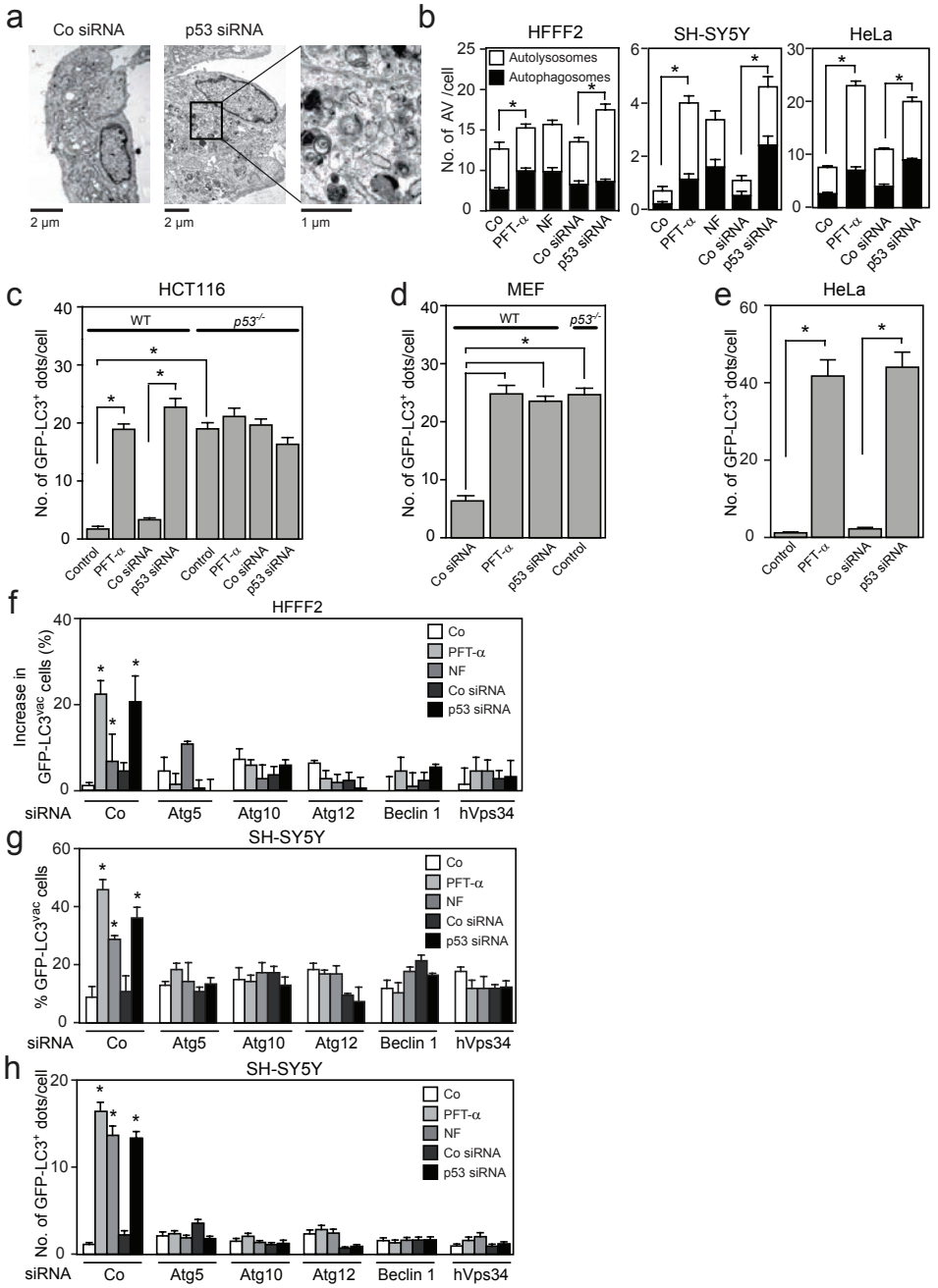

Figure S1 Induction of autophagy by p53 deletion, depletion or inhibition in multiple different cell lines. **(a**,**b)** Electron microscopic evidence for autophagy induction in human fetal fibroblasts (HFFF2), neuroblastoma (SH-SY5Y) and cervical carcinoma (HeLa) cells. Cells were transfected with a p53-specific or control siRNA (for 48 h) or exposed to PFT-α (30 µM, for 6 h) and then fixed and processed for transmission electron microscopy. Representative electron microphotographs are shown for HFFF2 in **a** and the frequency of immature (AV1) or mature (AV2) autophagic vacuoles for HFFF2, SH-SY5Y and HeLa cells (mean ± SEM, n = 50) is reported in **b**. Culture in nutrient-free (NF) conditions served as a positive control for autophagy induction. **(c-h)** The number of GFP-LC3 dots per cell is reported in HCT116 (**c**), MEF (**d**), HeLa (**e**) and SH-SY5Y (**h**) cells (mean ± SEM, n = 100 cells; * $p < 0.05$); the percentage of cells exhibiting the accumulation of GFP-LC3 in vacuoles (GFP-LC3^{vac}) is reported in HFFF2 (**f**) and SH-SY5Y (**g**) cells (mean ± SD of three independent experiments; Asterisks represent autophagy induction above background levels * $p < 0.05$). Cells of the indicated genotype were transfected with the indicated siRNAs for 24 h, then with GFP-LC3 for additional 24 h, and then left untreated or treated with PFT-α for 6 h, followed by the fixation, permeabilization and immunofluorescence microscopy.

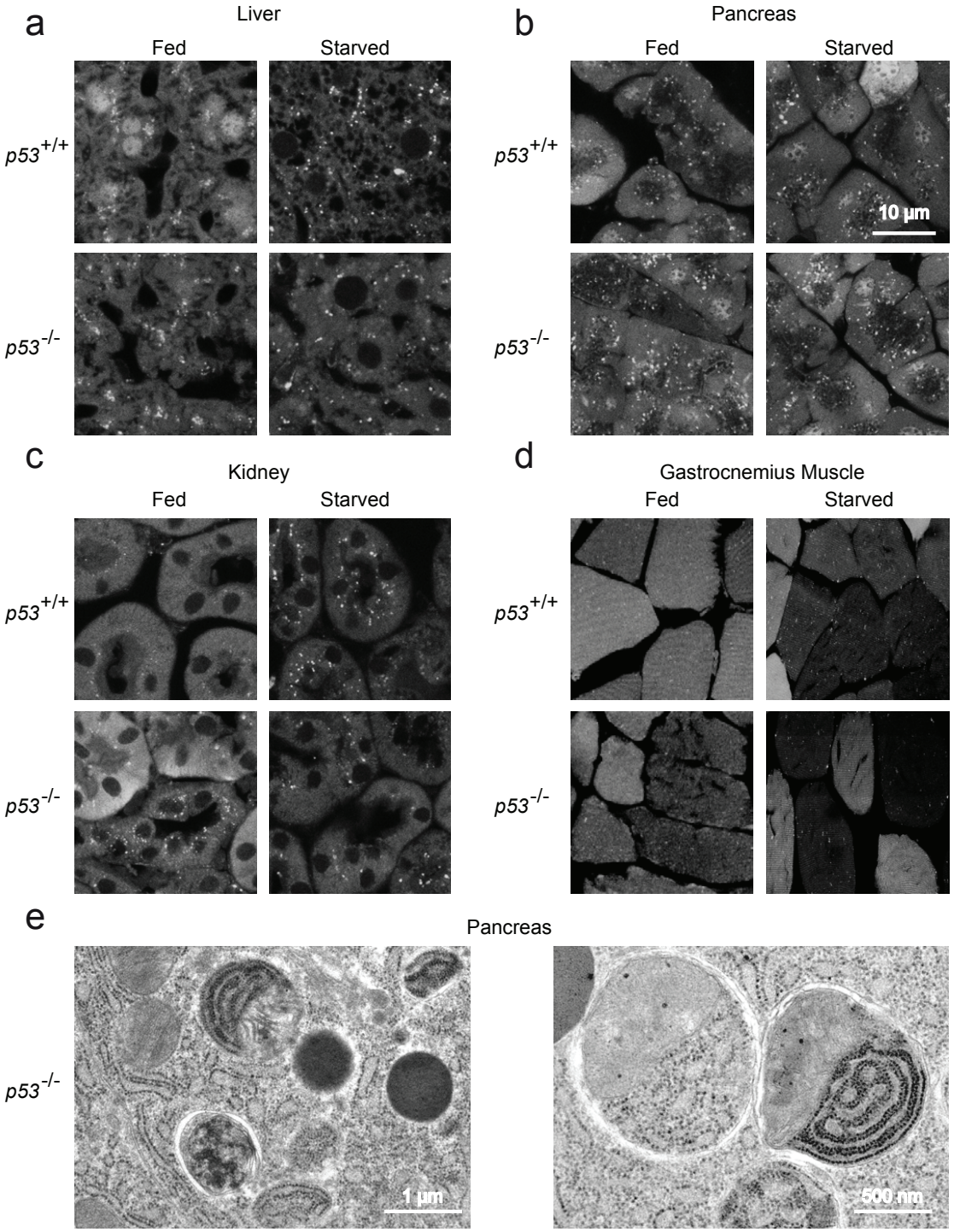

Figure S2 Histological evidence of autophagy in mice carrying a GFP-LC3 transgene on a *p53*$^{-/-}$ *versus* *p53*$^{+/+}$ background. Mice with the indicated genotype were anesthetized and tissues were fixed by perfusion, followed by confocal microscopy examination. Representative sections of the liver, exocrine pancreas, kidney glomeruli, and transverse sections of skeleton (gastrocnemius) muscle are shown in **a-d**. **(e)** Representative electronmicroscopic pictures from the exocrine pancreas of *p53*$^{-/-}$ mice are shown. Note the presence of mitochondria and rough ER in autophagosomes.

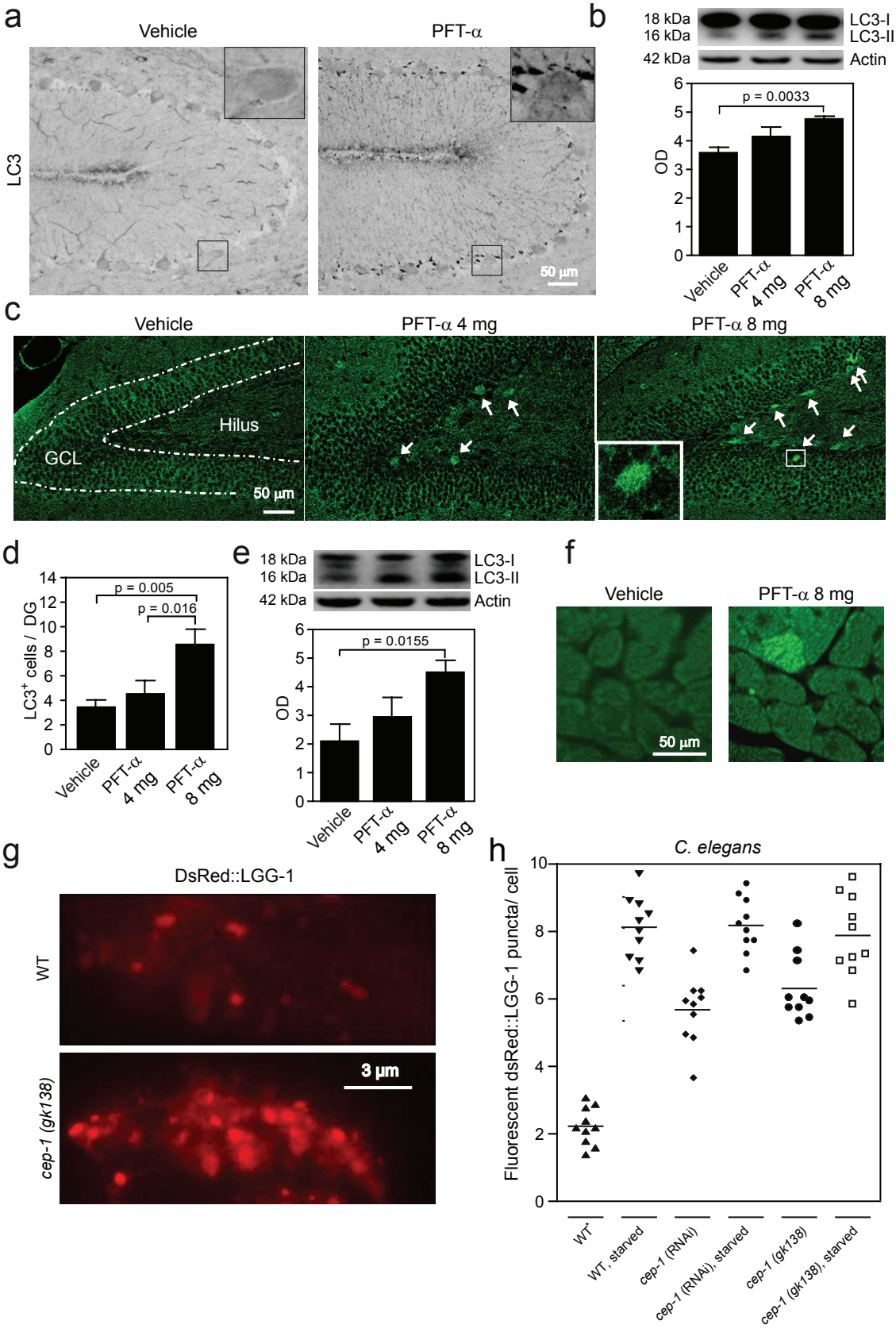
a
Vehicle
PFT-α
LC3
50 μm
b
18 kDa
16 kDa
LC3-I
LC3-II
42 kDa
Actin
p = 0.0033
OD
Vehicle
PFT-α 4 mg
PFT-α 8 mg
c
Vehicle
PFT-α 4 mg
PFT-α 8 mg
Hilus
GCL
50 μm
d
p = 0.005
p = 0.016
LC3+ cells / DG
Vehicle
PFT-α 4 mg
PFT-α 8 mg
e
18 kDa
16 kDa
LC3-I
LC3-II
42 kDa
Actin
p = 0.0155
OD
Vehicle
PFT-α 4 mg
PFT-α 8 mg
f
Vehicle
PFT-α 8 mg
50 μm
g
DsRed::LGG-1
WT
cep-1 (gk138)
3 μm
h
C. elegans
Fluorescent dsRed::LGG-1 puncta/ cell
WT
WT, starved
cep-1 (RNAi)
cep-1 (RNAi), starved
cep-1 (gk138)
cep-1 (gk138), starved

Figure S3 In vivo induction of autophagy. (**a**) Immunohistochemical detection of LC3 in the cerebellum after systemic injection of PFT-α. The upper panel is from the cerebellum of a vehicle treated mouse and the lower panel from a mouse treated with PFT-α. Five-month-old C57BL/6 male mice were injected twice (8 and 5 h before sacrifice) with PFT-α (total dose 8 mg/kg *i.p.*, two injections of 10 µl/g bodyweight of 0.4 mg/ml in saline containing 0.4 % DMSO) or vehicle alone, then deeply anesthetized with phenobarbital (50 mg/ml *i.p.*), perfused with ice cold PBS and immersion-fixed with 5 % formaldehyde. Brains were dehydrated with xylene and graded ethanol, paraffin-embedded and cut into 5 µm saggital sections. Sections were deparaffinized, and antigen retrieval was performed by boiling in 10 mM sodium citrate (pH 6) for 10 min. Nonspecific binding was blocked for 30 min with 4 % goat serum in PBS. Rabbit polyclonal anti-LC3 (Cell Signaling Technology) was added for 60 min at 20°C, followed by incubation with 2 µg/ml of a biotinylated goat anti-rabbit IgG diluted in PBS for additional 60 min. Visualization was performed using Vectastain ABC Elite (Vector Laboratories, Burlingame, USA). Note the increased, conspicuous staining of certain populations of cells located near to the large Purkinje cells. The inserts show higher magnifications of the squares in the pictures. (**b**). Immunoblot evidence for LC3 conversion induced by PFT-α *in vivo*, in the cerebellum. The cerebella of mice treated as in (a) with vehicle only, 4 or 8 mg PFT-α per kg bodyweight were homogenized and P2 (mitochondrial and synaptosomal) fractions were run on 4-12 % NuPAGE Bis-Tris gels (Novex) and transferred to reinforced nitrocellulose membranes (Schleicher & Schuell). The upper immunoblots shows immunoreactivity of LC3-I (18 kDa) and LC3-II (16 kDa). The lower immunoblot shows actin immunoreactivity, as a loading control. The column graph represents the densitometric quantification of the LC3-II bands from individual animals (n=4 per group), demonstrating a dose-dependent increase in LC3-II. **(c, d)**. Immunofluorescence detection of LC3 in the cerebellum after local and systemic PFT-α injection. Twenty-one-day-old mice treated were treated with vehicle or PFT-α as in (a, b) and received additional PFT-α via an intracerebroventricular (ICV) route (2x1 µg or 2x2 µg PFT-α for the 4 mg and 8 mg groups, respectively). The ICV PFT-α was administered using a syringe pump at a rate of 1 µl per minute, simultaneously with the intraperitonally administered PFT-α. All mice received an ICV injection volume of 5 µl of PFT-α solution or vehicle. The microphotographs in **(c)** show representative pictures of LC3 stainings from the dentate gyrus of mice treated with vehicle or an accumulated systemic dose of 4 mg or 8 mg of PFT-α. Cells with LC3 aggregates were located in the subgranular zone between granule cell layer (GCL) and the hilus, as indicated by arrows. The histograms in **(d)** represent the counts of strongly LC3-positive cells in the dentate gyrus (DG) of mice treated with vehicle or PFT-α as in (c) (n=4 per group). **(e)** Immunoblot evidence for LC3 conversion induced by PFT-α *in vivo*. Myocardia of mice treated with vehicle or PFT-α as in (a) were homogenized and P2 fractions were subjected to the immunoblot detection of LC3 as in (b). The densitometric quantification of LC3-II bands from individual animals (n=4 per group), demonstrated an increase in LC3-II induced by PFT-α. **(f)** Immunofluorescence detection of LC3 in the heart after systemic PFT-α injection. The myocardium (heart muscle) from mice treated with vehicle or PFT-α as in (a) was stained for LC3 immunoreactivity. The number of cells containing high levels of LC3 aggregates was lower in the myocardium of vehicle treated mice (left panel) than in mice treated with an accumulated PFT-α dose of 8 mg (right panel). **(g, h)**. Quantification of the punctuate distribution of the dsRED::LGG-1 fluorescent autophagosome marker in pharyngeal cells of adult *C. elegans* animals subjected to p53 depletion or deletion. Representative fluorescence microphotographs of adult pharyngeal cells with the indicated genotype and the indicated treatment are shown (**g**) and the LC3/LGG-1 fluorescent puncta per pharyngeal cell was quantitated (**h**). Each point represents one animal. Synchronous adult animal populations of the indicated genetic background were either fed ad libitum or starved (8 h). Experiments were performed at 20°C.

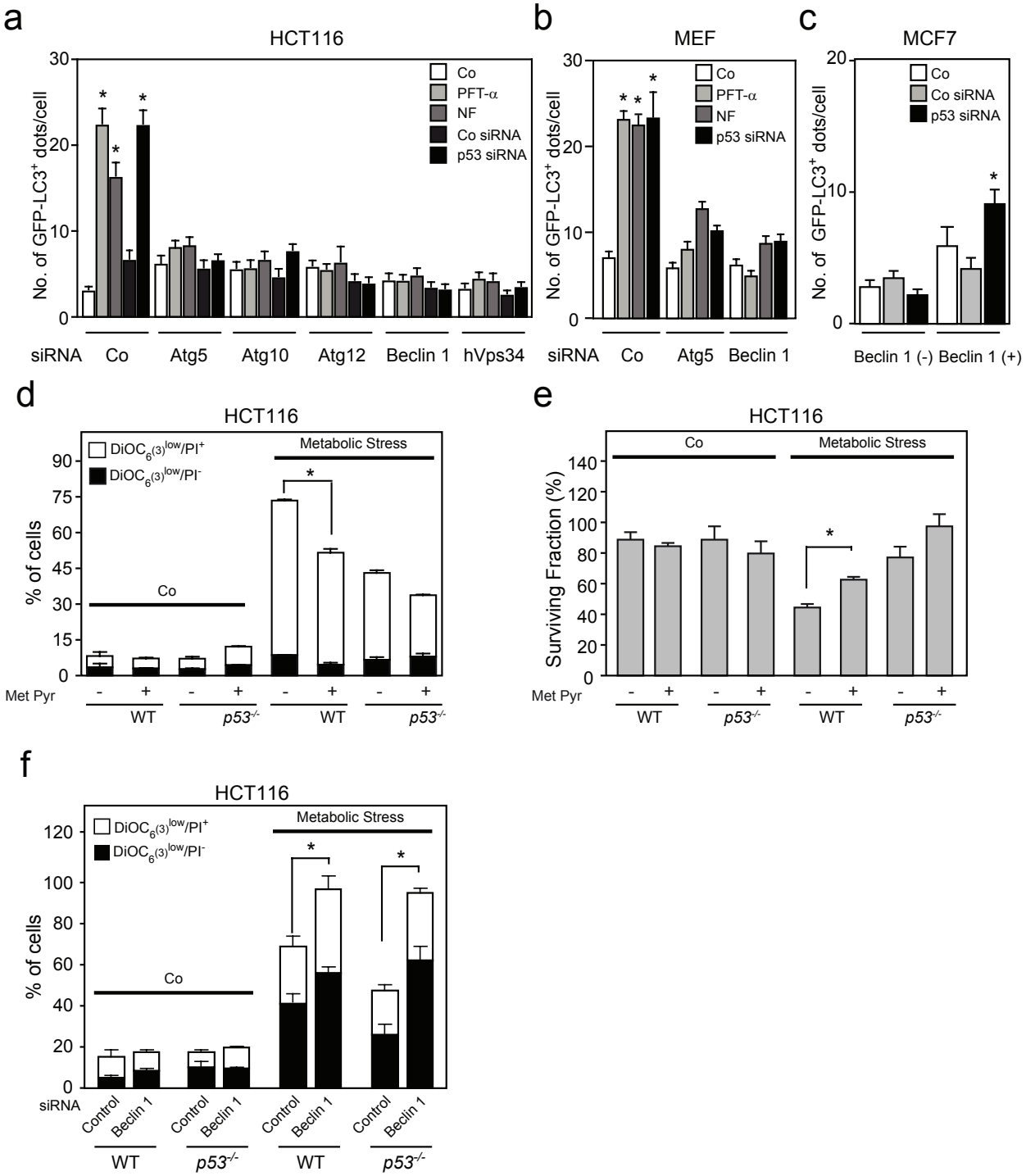

Figure S4 Autophagy and metabolism. The number of GFP-LC3 dots per cell is reported in HCT116 (**a**), MEF (**b**) and MCF7 (**c**) cells. Cells of the indicated genotype were transfected with the indicated siRNAs for 24 h, then with GFP-LC3 for additional 24 h, and then left untreated or treated with PFT-α for 6 h, followed by the fixation, permeabilization and immunofluorescence microscopy. Culture in nutrient-free (NF) conditions was used a control of autophagy induction. Data in are shown as mean ± SD of three independent experiments in which the number of GFP-LC3 dots per cells were counted for at least 100 cells. Asterisks represent autophagy induction above background levels ($p<0.01$). **(d,e,f)** Effect of p53 and autophagy on metabolic stress-induced cell death. WT or *p53*$^{-/-}$ HCT116 cells were left untreated or subjected to metabolic stress (48 h of culture in nutrient-free, hypoxic conditions) in the absence or in the presence of 10 mM methylpyruvate and then stained with $DiOC_6(3)$/PI for the cytofluorometric determination of apoptosis-associated parameters (**d**) or subjected to clonogenic survival assays (**f**). Alternatively, HCT116 cells were sham-transfected or transfected with control and Beclin 1-specific siRNAs and were subjected 48 later to metabolic stress and stained with $DiOC_6(3)$ and PI (**f**). Data in (**d,e**) are expressed as mean ± SD of 3 separate experiments. The black and white portions of the columns refer to the $DiOC_6(3)^{low}$ PI^- (dying) and $DiOC_6(3)^{low}$ PI^+ (dead) population, respectively.

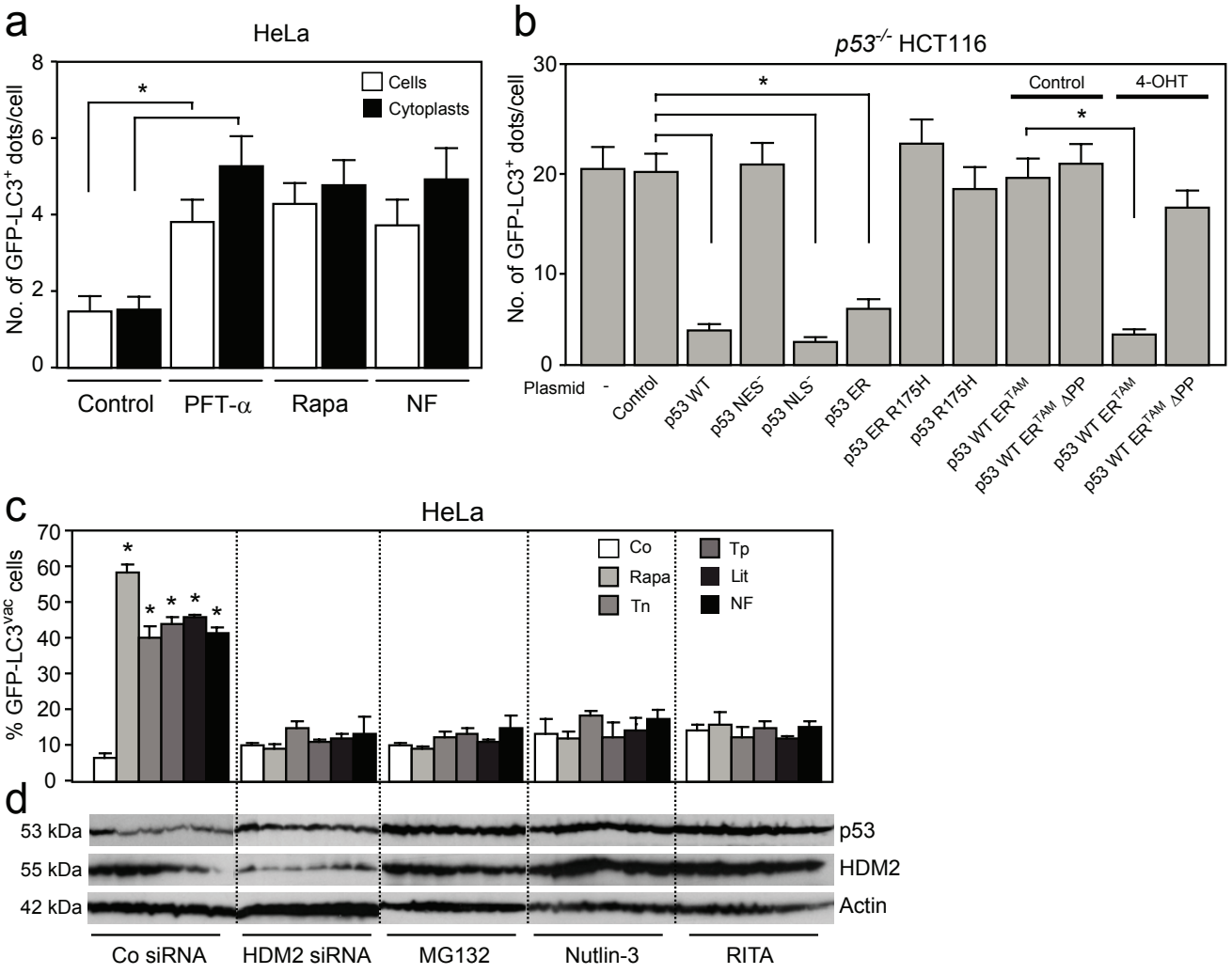

Figure S5: Mechanisms of autophagy regulation by p53. **(a)** The number of GFP-LC3 dots per cell is reported in HeLa cells and cytoplasts in the same conditions as in Figure 5b. Results are means ± SEM (n ≥100). **(b)** Effect of p53 mutants on autophagy in *p53*$^{-/-}$HCT116 cells, as determined in the same conditions as in Fig. 5e. GFP-LC3 dots per cell of p53$^{-/-}$ HCT116 cells transiently transfected with p53 mutants were quantified in **b** (mean ± SEM, n ≥100; * $p < 0.05$). **(c,d)** HeLa cells transfected with control or HDM2-targeted siRNAs were cultured in the presence or absence of MG132, Nutlin-3 or RITA for 3 h, followed by the treatment with autophagy inducers for 6 h. The percentage of cells exhibiting the accumulation of GFP-LC3 in vacuoles (GFP-LC3^{vac}) was quantified in **c**. The abundance of p53 and HDM2 was determined by immunoblotting assessments **(d).** Quantitations of GFP-LC3^{vac} cells in **c** are mean ± SD of three separate experiments. Asterisks represent autophagy induction above background levels ($p<0.01$). The blots shown in **b** are representative of 3 experiments.

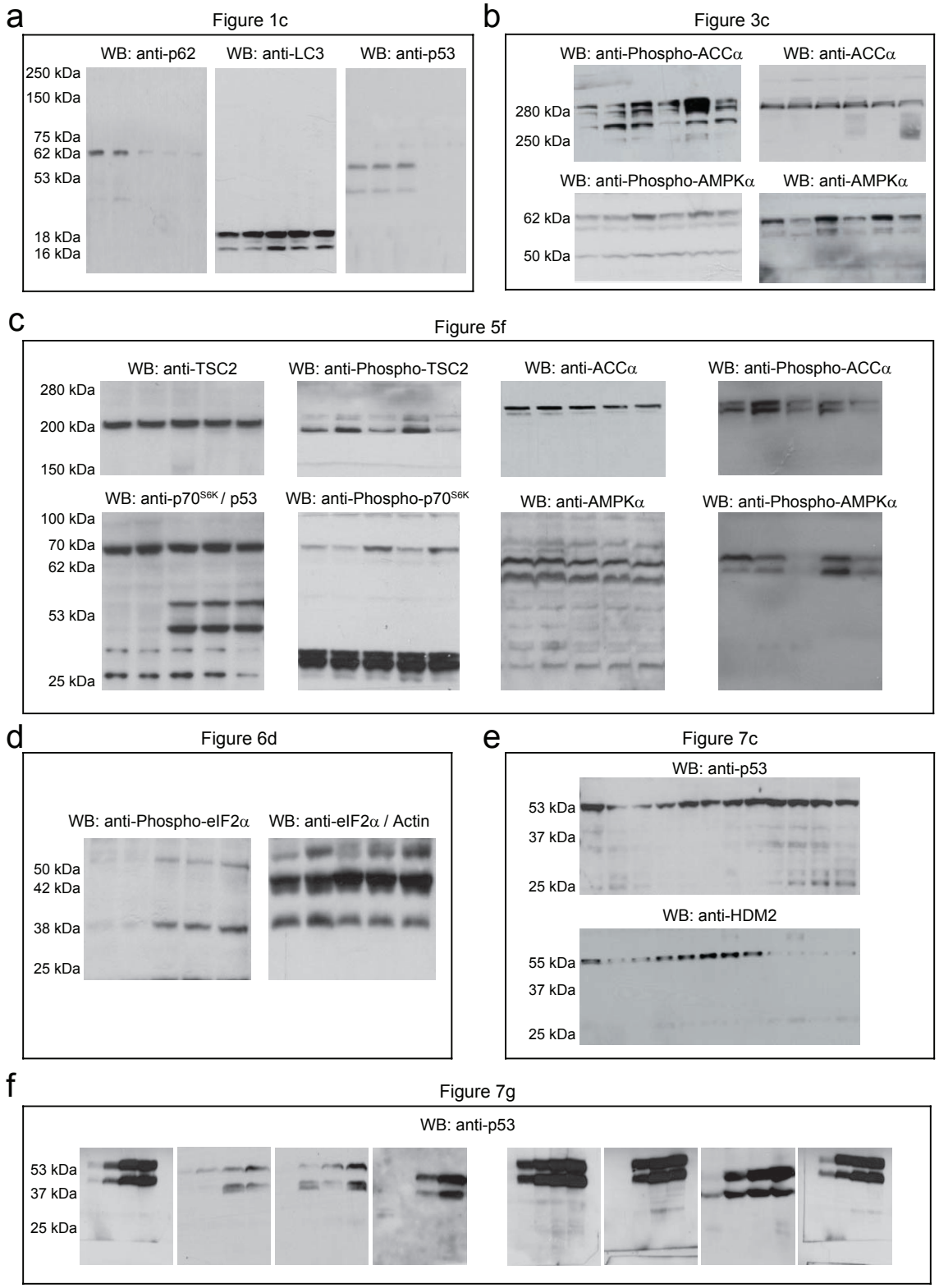

Figure S6: Large-scan images of some key blots.